ELECTRON-NUCLEAR DOUBLE RESONANCE OF F CENTERS IN KBr

S. S. ISHCHENKO, N. P. BARAN, M. F. DEĬGEN, M. A. RUBAN, V. V. TESLENKO, and V. V. UDOD

Institute of Semiconductors, USSR Academy of Sciences

Submitted March 26, 1969

Zh. Eksp. Teor. Fiz. 57, 763–773 (September, 1969)

The hyperfine and quadrupole interaction between F centers in KBr and nuclei of coordination spheres I – X of the crystal lattice are studied by the electron-nuclear double resonance (ENDOR) technique. The angular dependences of the ENDOR spectra are studied in detail at T = 20°K. A general form of the spin Hamiltonian is employed for the description of the experimental results; second-order perturbation theory, which turned out to be important for a number of spheres, was used in the diagonalization of the Hamiltonian. The hyperfine and quadrupole interaction between the F-center electron and the nuclei of the isotope K^{41} in sphere I is studied. The temperature dependence of the hyperfine and quadrupole constants is investigated in the 20 to 400°K temperature range. The dependence can be explained by the spin-phonon interaction.

1. INTRODUCTION

INVESTIGATIONS of the hyperfine[1)] interaction make it possible to measure directly the distribution of the wave function of a localized electron in a crystal. The data obtained thereby can be used to study different physical properties and to determine crystal parameters such as the structure of the conduction band, the effective masses of the electrons in the crystal[1], and others.

The most complete information on the hyperfine interaction of paramagnetic centers can be obtained by the method of electron-nuclear double resonance (ENDOR), which makes it possible to measure the hyperfine constants with a high degree of accuracy and with a sufficiently large number of lattice nuclei.

The F centers in KBr were investigated by the ENDOR method by Seidel[2] and by Holton and Blum[3]. The latter determined the constants of the magnetic hyperfine interaction of coordination spheres I, II, and IV at T = 1.3°K[3]. To interpret the experimental results for all spheres, a simplified spin-Hamiltonian with axial symmetry was used, and the quadrupole interaction was not investigated. KBr was investigated in greater detail by Seidel[2], who observed signals from spheres I–VIII, took into account the deviation of the spin Hamiltonian from axial symmetry, and measured the quadrupole interaction in spheres I, II, and IV. The measurements were made at T = 90°K; for spheres I, II, and IV he determined the constants also at T = 300°K. For some spheres, however, he was unable to determine all the spin-Hamiltonian parameters.

We have made a detailed investigation of the hyperfine, quadrupole, and spin-phonon interactions of the F centers in KBr. We determined the constants of the hyperfine interaction with nuclei of spheres I–X. We registered and measured the quadrupole interaction in all the spheres. To describe the experimental results, we used a common form of the spin Hamiltonian. A detailed description of the angular dependences of the ENDOR lines in both the hyperfine and in the quadrupole interactions was possible only when account was taken of the corrections that must be added to the resonant frequencies in second order perturbation theory[4]. The temperature dependence of the hyperfine and quadrupole interaction constants was investigated in a wide range of temperatures, and was explained on the basis of the concept of spin-phonon interaction. The hyperfine and quadrupole interactions of the F-center electron with the nuclei of sphere I of the low-abundance isotope K^{41} were investigated in detail.

[1)] By "hyperfine" is meant here the magnetic interaction of the electron spin with the crystal-lattice nuclei.

2. EXPERIMENTAL PROCEDURE AND TECHNIQUE

We used for the measurements single crystals of KBr grown by the Kyropoulos method in air. The F centers were obtained by electrolytic coloring. The concentration of the F centers in the optical measurements was 10^{18} cm^{-3}. The investigations were performed with a superheterodyne ENDOR spectrometer operating in the three-cm band (ν_{microw} = 9290 MHz)[5]. The devices used to operate at low and high temperatures are described in[6,7]. The sample was rotated in the (001) plane.

3. EXPERIMENTAL RESULTS AND DISCUSSION

To describe the experimental results we used the spin Hamiltonian of the lattice nucleus in an external constant magnetic field H with allowance for the hyperfine and quadrupole interactions with the localized electron

$$\hat{\mathcal{H}} = -\frac{\mu_{nuc}}{I}\mathbf{H}\hat{\mathbf{I}} + a\hat{\mathbf{I}}\hat{\mathbf{S}} + \sum_{p,q}(D_{pq}\hat{I}_p\hat{I}_q + Q_{pq}\hat{I}_p\hat{I}_q), \qquad (1)$$

where a is the constant of the isotropic hyperfine interaction, equal to

$$a = \frac{8\pi}{3}\frac{\mu\mu_{nuc}}{SI}|\psi(\rho=0)|^2, \qquad (2)$$

and the tensor components of the anisotropic hyperfine and quadrupole interactions are

$$D_{pq} = \frac{\mu\mu_{nuc}}{SI}\int|\psi|^2\frac{3x_px_q-\delta_{pq}\rho^2}{\rho^5}dV, \qquad (3)$$

$$Q_{pq} = \frac{eQ_0}{2I(2I-1)}\left(\frac{1}{3}\delta_{pq}-1\right)\frac{\partial^2 v}{\partial x_p\partial x_q}.$$

We used a local system of coordinates with origin at the nucleus; ψ is the wave function of the localized electron and ρ its radius vector; S, I, μ and μ_{nuc} are respectively the spins and magnetic moments of the electron and nucleus; Q_0 is the quadrupole moment of the nucleus and z the potential of the electric field at the location of the nucleus; p and q number the axes of a rectangular coordinate system. The spin Hamiltonian was simplified in accordance with the symmetry that holds for nuclei of the various coordination spheres. For a complete description of the ENDOR spectra and their angular dependences in spheres I and IV, and also for interaction with the isotope K^{41}, second order perturbation theory was taken into account in the diagonalization of the spin Hamiltonian.

Spheres I, II, III. The interaction of the F-center electron with the nuclei of sphere I of the principal isotope K^{39} is described only by using the so-called second-order corrections. The latter are taken to mean the energy corrections that arise in the second perturbation-theory approximation with the hyperfine interaction as the perturbation and with the electronic Zeeman energy as the zero-order Hamiltonian ("indirect" interaction of the nuclei), corrections connected with the allowance for the deviation of the nuclear-spin quantization axis from the direction of the external magnetic field H (motion of the nuclear movement in an effective field), and corrections due to the quadrupole interaction with account taken of the second order of perturbation theory (the latter is manifest in the asymmetry of the quadrupole triplet)[4]. Indirect interaction of the nuclei leads to additional splittings of the spectral lines (second-order structure), and the effective field and quadrupole interaction in second order of perturbation theory lead only to a shift of the frequencies of the observed transitions, causing in a number of cases appreciable deviations from the angular dependences obtained when the customary formulas are used. The ENDOR lines from the nuclei of sphere I of K^{39} reveal a second-order structure. The experimental spectrum, and also the angular dependences, are completely described by formulas that take into account the aforementioned corrections[4].

A detailed study of the angular dependences of this and succeeding spheres was made at T = 20°K, but the hyperfine and quadrupole constants were determined in a wide temperature interval (in many cases 20–400°K). The measurement results are given in the table. A discussion of the temperature dependences of the hyperfine and quadrupole constants and a comparison with theory will be presented after the description of the experimental results.

In sphere II, experiment reveals ENDOR signals from two isotopes, Br^{79} and Br^{81}, which have approximately the same natural abundance. For this as well as for the succeeding spheres, we investigated the angular dependences of the resonant frequencies for both isotopes, but the positions of the lines, and also hyperfine and quadrupole constants, were recalculated within the limits of experimental error in terms of the ratios of the corresponding moments (magnetic and quadrupole). The table therefore lists the results of the measurements (with the exception of sphere X) only for Br^{81}.

Constants of hyperfine and quadrupole interactions of F centers in KBr

Sphere, type of nucleus	a, MHz	b_1, MHz	b_2, MHz	Q', MHz	Q'', MHz	φ, deg	φ', deg	T, °K
I, K^{39}	18.228	0.769		0.190				20
	18.322	0.768		0.186				77
	18.834	0.726		0.182				300
	18.852	0.720		0.180				340
I, K^{41}	10.042	0.422		0.234				20
	10.086	0.418		0.230				77
II, Br^{81}	42.740	2.740	0.073	0.220				20
	42.870	2.680	0.053	0.220				77
III, K^{39}	0.262	0.022		$\leqslant$0.001				20
	0.274	0.022		$\leqslant$0.001				77
IV, Br^{81}	5.716	0.411		0.112				20
	5.736	0.409		0.106				77
	5.862	0.401		0.064				300
	5.890	0.401		0.058				340
	5.900	0.400		0.049				370
V, K^{39}	0.153	0.013	0.0005	±0.003	∓0.0004	15	5	20
	0.153	0.013	0.0005	±0.003	∓0.0004	15	5	77
VI, Br^{81}	0.820	0.088	0.011	±0.023	∓0.010	34.5	35	20
	0.844	0.087	0.002	±0.023	∓0.010	34.8	35	77
VIII, Br^{81}	0.540	0.064	0.001	0.009				20
	0.546	0.064	0.001					77
X, Br^{81}	0.158	0.028	−0.0008	0.020		19,3		20
X, Br^{79}	0.150	0.027	−0.0007	0.024		19,7		20
(IXa), K^{39}	(0.035)							20
(XII), Br^{81}	(0.030)							20

Note. The error in the experimental results did not exceed the following values: a – 0.010 MHz, b_1, b_2–0.05 MHz, and Q′ – 0.003 MHz, for spheres I and II, and a–0.005 MHz, b_1 and b_2– 0.003 MHz, Q′ and Q″– 0.001 MHz, φ – 2°, and φ' – 4° for spheres III – X.

The parentheses indicate inexact results. The directions of the principal axes of the anisotropic hyperfine and quadrupole interaction tensors are the same as in [6]. The angles φ and φ' define the direction of the principal axes of the tensors for spheres with symmetry C_s.

The magnetic moment of both Br isotopes is much larger than the magnetic moment of K^{39}. In this connection, the hyperfine constants of sphere II are larger (by approximately 2.3 times) than the corresponding constants of sphere I, although the nuclei of sphere II lie farther from the defect. The constants of the remaining spheres are much smaller. We can therefore conclude that the main contribution to the line width of electron paramagnetic resonance (EPR) is made by the hyperfine interaction of the F-center electron with the nuclei of the first two spheres.

The ENDOR lines of sphere II are strongly broadened, this being apparently due to the unresolved second-order structure connected with the indirect interaction of the nuclei. In determining the constants of sphere II, and also of other spheres, where no account was taken of second-order defects, we used the general formula for the ENDOR frequencies in the first approximation of perturbation theory[2)]:

$$h\nu = h\nu_L + {}^1/_2\{a + b_1(3\cos^2\vartheta - 1) + b_2(3\cos^2\vartheta_1 - 1) - \\ - (2m-1)[(Q'+Q'')(3\cos^2\vartheta' - 1) + 2Q''(3\cos^2\vartheta_1' - 1)]\}, \quad (5)$$

where $b_1 = -{}^1/_3(D_{11} + 2D_{22})$, $b_2 = {}^1/_3(D_{11} - D_{22})$,

$$Q' = {}^9/_4 Q_{33}, \quad Q'' = {}^3/_4(Q_{11} - Q_{22}),$$

2) Formula (2) has been written out for the summary frequencies (M = ½, M is the eigenvalue of the electron spin projection operator).

In the case of axial symmetry (spheres I, III, IV, IXa) we have $\vartheta' = \vartheta$, $\vartheta_1' = \vartheta_1$, $b_2 = Q'' = 0$. For the simplifying symmetry group C_{2v} (spheres II and VIII), only the equations $\vartheta' = \vartheta$ and $\vartheta_1' = \vartheta_1$ are valid.

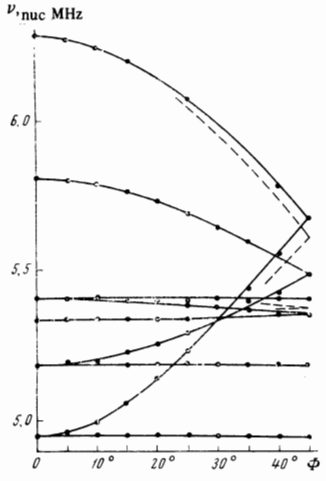

FIG. 1. Angular dependence of the ENDOR spectrum of K^{41} nuclei of sphere I. All the angular dependence and spectra shown in the figures were obtained at T = 20° K.

ϑ and ϑ_1 are respectively the angles between the magnetic field and the principal axes 3 and 1 of the hyperfine interaction tensor; ϑ' and ϑ_1' are the same angles for the quadrupole tensor, ν_L is the nuclear Larmor frequency, m is the eigenvalue of the nuclear spin-projection operator (it is necessary to substitute in (5) the larger of the two values corresponding to the transition with $\Delta m = \pm 1$). The constant Q′ was determined from the upper quadrupole triplet at $\vartheta = 0°$, where the quadrupole splitting is maximal and equal to 2Q′. The constant Q″ was not determined, owing to the poor resolution of the quadrupole interaction for the other lines.

For sphere III, which consists of K^{39} nuclei, the theory contains three parameters: a, b_1, and Q′. When the sample is rotated in the (001) plane, the spectrum consists of two lines. The second-order effects referred to above are small in this case and are not revealed in the experiment. No quadrupole splitting was observed, but from a comparison of the change of the line width with the angular dependence of the quadrupole interaction it is possible to estimate that $Q' \leq 0.001$ MHz.

Sphere I of K^{41} nuclei. The ENDOR spectrum due to the interaction of the F-center electron with the nuclei of the isotope K^{41} in sphere I was observed by Seidel[2]; however, the angular dependence of the ENDOR lines was not investigated. It turned out at the same time that it is poorly described by the usual formula (5). Since the natural abundance of the isotope K^{41} is relatively small (6.9%), it is most probable that sphere I contains only one K^{41} nucleus. This is confirmed by the experimental spectrum, whose lines reveal no second-order structure connected with the indirect interaction of the nuclei and are quite narrow. However, the values of the constants in this case are such that the remaining second-order corrections are appreciable and distort strongly the angular dependence of the ENDOR lines. As shown in[8], where an analogous problem was solved for F centers in KCl, it is possible to use in this case a single-particle effective spin Hamiltonian, simplifying it in accordance with the existing symmetry. The ENDOR frequencies for this case will be

$$\nu_{M,m} = |M\Delta_M - B' + (\bar{Q}_0 - 2MB)(2m-1) + \frac{Q'^2}{8M\Delta_M}\{[2I(I+1) - 3(2m^2-2m+1)]\sin^4\alpha + [8(3m^2-3m+1) - 4I(I+1)+1]\sin^2 2\alpha\}|, \quad (6)$$

$$\Delta_M = \left[\left(a - b_1 - \frac{\nu_L}{M}\right)^2 \sin^2\vartheta + \left(a + 2b_1 - \frac{\nu_L}{M}\right)^2 \cos^2\vartheta\right]^{1/2}, \quad (7)$$

where

$$\bar{Q}_0 = \frac{1}{2}Q'(3\cos^2\alpha - 1), \quad (8)$$

$$\cos^2\alpha = \left(1 + \frac{2b_1 - \nu_L/M}{a}\right)^2 \left[\left(1 - \frac{b_1 + \nu_L/M}{a}\right)^2 \sin^2\vartheta + \left(1 + \frac{2b_1 - \nu_L/M}{a}\right)^2 \cos^2\vartheta\right]^{-1} \cos^2\vartheta, \quad (9)$$

$$B' \approx B \approx \frac{a^2}{4\nu_0}\left[1 - \frac{b}{a}(3\cos^2\vartheta - 1)\right]. \quad (10)$$

In (10), B and B′ are given accurate to terms $\sim b^2/4\nu_0$, which are not significant in our case (ν_0—electron Larmor frequency); exact expressions are given in[4].

Figure 1 shows the angular dependence of the summary ENDOR frequencies of sphere I of K^{41}. (Here and in the succeeding figures the solid lines are theoretical the points represent the experimental data, Φ is the angle between the field H and the [100] axis in the (001) plane, and ν_{nuc} is the frequency of the generator that induces the nuclear transitions.) The dashed lines represent the theoretical curves for the angular dependences of a number of frequencies without allowance for the second-order corrections. The absence of experimental points from the upper curve at certain orientations is due to the overlap of the corresponding ENDOR line by the stronger lines of sphere IV. Figure 2 illustrates the ENDOR spectrum of sphere I of K^{41} at $\Phi = 45°$; 4—9 are the summary frequencies, and 1—3 represents part of the spectrum of the difference frequencies.

Sphere IV. Figure 3 shows the angular dependence of the ENDOR frequencies of sphere IV. The indirect interaction of the nuclei is small in this case, owing to the smallness of the constant a, and does not appear in the experiment; the remaining second-order corrections are appreciable. Therefore the angular dependences, in analogy with the interaction with K^{41}, are completely described only when formula (6) is used. As seen from Fig. 3, good agreement is obtained in

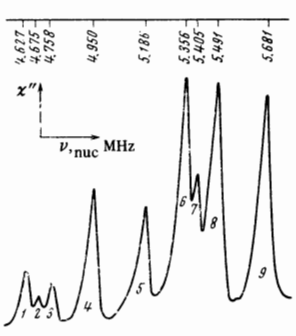

FIG. 2

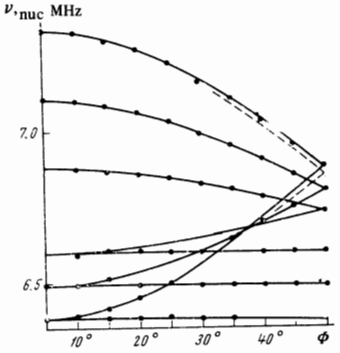

FIG. 3

FIG. 2. ENDOR spectrum for K^{41} nuclei of sphere I, $\Phi = 45°$. In this and in the succeeding figures χ″ is the chemical part of the paramagnetic susceptibility.

FIG. 3. Angular dependence of the summary ENDOR frequencies of the Br^{81} nuclei of sphere IV.

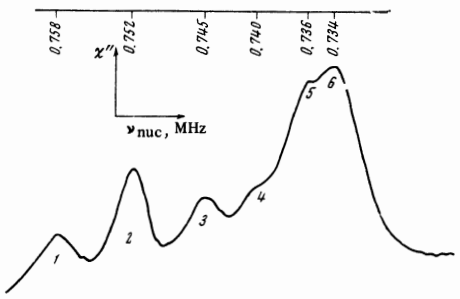

FIG. 4. Spectrum of Summary ENDOR spectrum of the K^{39} nuclei of sphere V, $\Phi = 0°$.

this case between theory and experiment, whereas the discarding of the second-approximation corrections leads to a noticeable discrepancy (dashed lines).

Sphere V. The ENDOR lines from the nuclei of sphere V of K^{39} were observed in[2]; however, the angular dependence of the frequencies was not investigated, and not all the spin-Hamiltonian parameters were determined. To describe the interaction with this sphere, a simplified spin Hamiltonian of axial symmetry was used in[2]. The ENDOR spectrum of sphere V observed by us has made it possible to describe the experimental results by using the general form of the Hamiltonian, and to determine all its parameters. The angular dependences of the ENDOR frequencies were also determined. Figure 4 shows one of the spectra of sphere v at $\Phi = 0°$. Besides the principal lines (2, 5, 6) there were registered additional ines (1, 3, 4) apparently due to the quadrupole interaction in sphere V. The arguments favoring this assumption are as follows: when $\Phi = 0°$, a distinct triplet is observed, in which the two additional lines (1, 3) are symmetrical with respect to the fundamental frequency (2); all the additional lines are broader and less intense compared with the fundamental lines of sphere V, as is usually observed also in quadrupole triplets owing to the statistical scatter of the local electric fields at the different nuclei; the angular dependence of the additional lines in those sections where it could be traced corresponds to the angular dependence of the quadrupole interaction; all the observed lines can be described by the formulas for the frequencies of sphere V with account taken of the quadrupole interaction[3]. Second-order effects for the sphere under consideration, and also for the more remote spheres, are negligible as the result of the smallness of the constants and do not appear in the experiment; formula (5) was therefore used in the reduction of the experimental results.

Figure 5 illustrates the angular dependences of the ENDOR frequencies of sphere V. The circles denote the experimental points, from which the quadrupole constants were determined, and the squares denote the points from which the hyperfine constants were determined. The dashed lines show the theoretical curves corresponding to the quadrupole interaction. Since the total angular dependence greatly complicates the figure, we show for the quadrupole interaction only those curves for which experimental lines were observed. The vertical segments passing through the points show the broadening of the corresponding ENDOR lines.

Spheres VI and VIII. Figure 6 shows the ENDOR spectrum of the nuclei of coordination spheres VI and VIII. Lines 1—5 belong to sphere VI of Br^{81}, 6—8 to sphere VIII of Br^{81}, and 9—13 to sphere VI of Br^{79}. Quadrupole interaction was registered and measured also in these spheres. Favoring the argument that the observed lines correspond to quadrupole interaction are all the considerations advanced for the case of sphere V. In addition, quadrupole splittings for the isotopes Br^{79} and Br^{81} can be recalculated in terms of the ratios of the quadrupole moments of the corresponding nuclei. Lines 1 and 9 in Fig. 6 correspond to the quadrupole interaction of Br^{81} and Br^{79} respectively in sphere VI. In sphere VIII, the quadrupole interaction has not been resolved for the given orientation. In sphere VI, the quadrupole splitting for several lines is clearly observed in the entire range of angles, so that all the parameters of the spin Hamiltonian describing the quadrupole and hyperfine interactions could be determined.

For sphere VIII, it is impossible to trace completely the angular dependence of the quadrupole interaction; we therefore use the axial-symmetry spin Hamiltonian for its description. The magnetic hyperfine interaction was described by the general spin Hamiltonian.

Sphere X. In addition to the spheres indicated above, we noted also two groups of ENDOR lines located near the Larmor nuclear frequencies of Br^{81} and Br^{79}. The angular dependence of these lines, which can be traced quite clearly in the entire investigated angle range, has made it possible to identify the difference frequencies of Br^{81} and the summary frequencies of Br^{79} of sphere X. The summary frequencies Br^{81} and the difference frequencies of Br^{79} are almost completely overlapped by the stronger lines of spheres VI and VIII, and appear only at certain orientations.

It should be noted that the interpretation of the signals from the nuclei of the remote spheres entails certain difficulties, which were pointed out in earlier papers on ENDOR[9,10,11]. Therefore the identification of the lines of the remote spheres is most frequently less reliable than that of the nearby spheres. In the present case, however, the lines of sphere X were

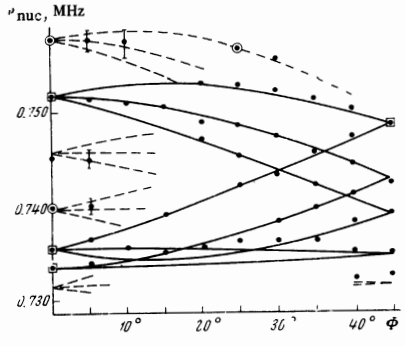

FIG. 5. Angular dependence of the ENDOR spectrum of the K^{39} nuclei of sphere V.

[3] The considerations presented here with respect to the quadrupole interaction were first pointed out by Kersten [10], who also called our attention to the need for revealing the interpretation of the coordination spheres IXa and XIII in KCl [6].

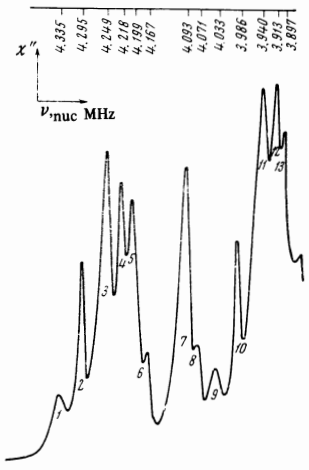

FIG. 6

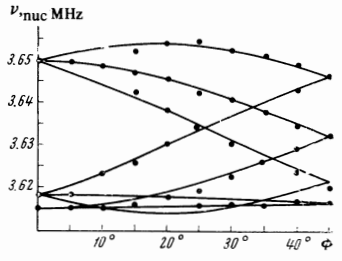

FIG. 7

FIG. 6. Spectrum of summary ENDOR lines of Br^{81} and Br^{79} nuclei of sphere VI and of Br^{81} of sphere VIII, $\Phi = 45°$.

FIG. 7. Angular dependence of the summary ENDOR frequencies of Br^{79} of sphere X.

observed in a clean region and the clearly traced angular dependence makes it possible to regard the interpretation as perfectly reliable.

The angular dependence of the summary frequencies of Br^{79} of sphere X, which was investigated in greatest detail in the experiment, is shown in Fig. 7. All the parameters of the spin Hamiltonian that describes the magnetic hyperfine interaction have been determined. Figure 8 illustrates the ENDOR spectrum of the sphere X at $\Phi = 0°$, with (4—6) denoting the summary lines of Br^{79}, (1) one of the difference lines of Br^{81}, and (7, 8) the difference lines of sphere VIII of Br^{81}. Additional lines (2, 3) were also observed. The frequency distances between lines (1—2) and (3—4) can be expressed in terms of each other via the ratios of the quadrupole moments; these lines are broader and less intense. We have therefore attributed the observed lines to the quadrupole interaction in sphere X. Since the total angular dependence of these additional lines was not traced, we used for their description the simplified spin Hamiltonian of the axial-symmetry quadrupole interaction.

Spheres IXa and XII. Near the nuclear Larmor frequencies of K^{39} and Br^{81}, we observed also ENDOR lines due apparently to more remote spheres. The weak intensity and the strong overlap of the lines in the spectra do not make it possible to interpret these interactions uniquely. However, a qualitative comparison of the experimental angular dependences of the observed lines with the theoretical angular dependences of the succeeding spheres makes it possible apparently to give preference to the coordination spheres IXa and XIII. Neglecting the contribution of the anisotropic hyperfine interaction, we have estimated the isotropic constant a for these spheres.

Temperature dependence of the hyperfine interaction and quadrupole interaction constants. The investigation of the temperature dependences of the hyperfine and quadrupole interaction constants was carried out for spheres I—VIII. The interaction was investigated in greatest detail in a wide temperature interval (20—400°K) for spheres I and IV, where the observed temperature dependence is strongest. In the remaining spheres, the constants were determined at values of T equal to 20 and 77°K. In all the investigated spheres, the constant a increased with increasing temperature, and b and Q decreased[4]. The change of the constant a did not exceed 3% in the investigated temperature interval, the change of b in sphere I was maximal and amounted to 6%; nor did it exceed 3% in the remaining spheres. The sharpest temperature dependence of the quadrupole constant Q was observed in sphere IV (55%), while in the remaining spheres the change did not exceed 6%.

The observed temperature dependence was interpreted on the basis of the concepts of spin-phonon interaction[7]. To find the theoretical temperature dependence, the hyperfine and quadrupole interaction constants were expanded in a series in terms of the independent differences of the displacements u_l of the nucleus under consideration and of the lattice nuclei (l numbers the lattice nuclei). Averaging the obtained expressions over all the phonons and using the Debye approximation, we can obtain the following expressions for the measured constants:

$$\begin{aligned} a(T) &\approx a^{(0)} + a^{(2)}\langle u_l^2\rangle, \\ b(T) &\approx b^{(0)} + b^{(2)}\langle u_l^2\rangle, \\ Q(T) &\approx Q^{(0)} + Q^{(2)}\langle u_l^2\rangle, \end{aligned} \tag{11}$$

where

$$\langle u_l^2\rangle = \frac{18\hbar}{M_1\omega_D^3}\int_0^{\omega_D}\left(\frac{1}{e^{\hbar\omega/kT}-1}+\frac{1}{2}\right)\omega^2 d\omega =$$

$$= \frac{18\hbar^2}{M_1 k\Theta}\int_0^1\left(\frac{1}{e^{\Theta/tT}-1}+\frac{1}{2}\right)t\,dt, \tag{12}$$

$$a^{(2)} \equiv \frac{1}{2}\sum_l\left(\frac{\partial^2 a}{\partial u_l^2}\right),\quad b^{(2)} \equiv \frac{1}{2}\sum_l\left(\frac{\partial^2 b}{\partial u_l^2}\right), \tag{13}$$

$$Q^{(2)} \equiv \frac{1}{2}\sum_l\left(\frac{\partial^2 Q}{\partial u_l^2}\right)$$

ω_D is the Debye frequency, Θ is the Debye temperature, k is Boltzmann's constant, $M_1 = (M_+ + M_-)/2$, M_+ and M_- are the masses of the positive and negative ions respectively, and $a^{(0)}$, $b^{(0)}$, and $Q^{(0)}$ are the constants of the hyperfine and quadrupole interactions in the rigid lattice.

Figure 9 illustrates the comparison of theory with experiment for sphere IV. The parameters of the theory were determined from the experimental points at values of T equal to 20 and 300°K[5]:

$$a^{(0)} = 5.687\ \text{MHz} \qquad Q^{(0)} = 0.122\ \text{MHz}$$
$$a^{(2)} = 1.415\ \text{MHz/Å}^2, \qquad Q^{(2)} = -0.465\ \text{MHz/Å}^2.$$

The determined parameters characterize the spin-phonon interaction in the crystal and can be used to determine the F-center relaxation times.

The results show that the square of the modulus of the wave function of the F-center electron, obtained

[4] By b and Q is meant any of the constants b_1 or b_2 and Q′ or Q″, respectively.

[5] We note that in the case of strong temperature dependence (as is the case for quadrupole interaction in the spheres IV), it would be necessary to take into account in the expressions (11) also terms of higher order.

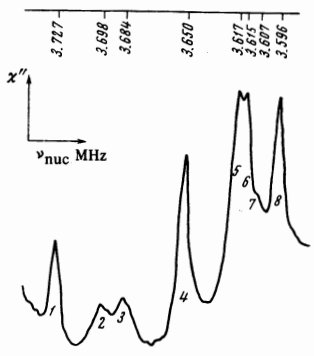

FIG. 8

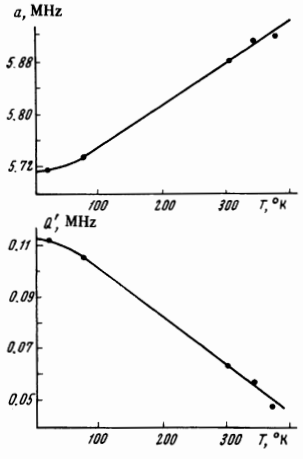

FIG. 9

FIG. 8. ENDOR spectrum of sphere X, Φ = 0°.

FIG. 9. Temperature dependence of the isotropic hyperfine interaction constant (a) and of the quadrupole interaction (Q). Solid lines– theory (formulas (11)), points – experimental data.

from the isotropic hyperfine constant, decreases monotonically in KBr with increasing distance from the defect. This dependence is close to exponential. The latter indicates, apparently, that the anisotropy of the band-electron effective-mass tensor components is small. The structure of the conduction band and of the effective-mass tensor will be investigated in greater detail on the basis of the obtained data by the method developed in[1].

[1] V. G. Grachev and M. F. Deigen, and S. I. Pekar, Fiz. Tverd. Tela 9, 3157 (1967) [Sov. Phys.-Solid State 9, 2489 (1968)].

[2] H. Seidel, Z. Physik 165, 218 (1961).

[3] W. C. Holton and H. Blum, Phys. Rev. 125, 89 (1962).

[4] V. Ya. Zevin, S. S. Ishchenko, and M. A. Ruban, Zh. Eksp. Teor. Fiz. 55, 2108 (1968) [Sov. Phys.-JETP 28, 1116 (1969)].

[5] M. F. Deĭgen, M. A. Ruban, and Yu. S. Gromovoĭ, Fiz. Tverd. Tela 8, 826 (1966) [Sov. Phys. Solid State 8, 662 (1966)].

[6] M. F. Deĭgen, M. A. Ruban, S. S. Ishchenko, and N. P. Baran, Zh. Eksp. Teor. Fiz. 51, 1014 (1966) [Sov. Phys.-JETP 24, 676 (1967)].

[7] N. P. Baran, V. V. Grachev, M. F. Deĭgen, and S. S. Ishchenko, ibid. 55, 2069 (1968) [28, 1094 (1969)].

[8] N. P. Baran, M. F. Deĭgen, V. Ya. Zevin, and M. A. Ruban, Fiz. Tverd. Tela 10, 3342 (1968) [Sov. Phys.-Solid State 10, 2640 (1969)].

[9] R. Kersten, Phys. Stat. Sol. 29, 575 (1968).

[10] W. T. Doyle, Phys. Rev. 131, 555 (1963).

[11] S. S. Ishchenko, N. P. Baran, M. F. Deĭgen, and M. A. Ruban, ZhETF Pis. Red. 7, 122 (1968) [JETP Lett. 7, 93 (1968)].

Translated by J. G. Adashko
87

As a rule, all the photographs were obtained in an increasing magnetic field intensity.

RESULTS

The variation of the diffraction pattern as a function of the magnetic field intensity in the paramagnetic (300°K), antiferromagnetic (145°K), and ferromagnetic (77°K) regions are shown in Fig. 2.

In the paramagnetic region, no noticeable change is observed in the x-ray interference intensity as a function of the magnetic field intensity.

In the antiferromagnetic region, in fields 0—9 kOe, there are likewise no changes in the form of the x-ray patterns, but in a field of ~10 kOe the diffraction pattern changes appreciably: all the x-ray lines shift noticeably, the diffraction peak from the plane $(210)_h$[2] splits into two components. The splitting of the $(210)_h$ line is evidence of a lowering of the symmetry of the crystal lattice to rhombic[4]. It is seen from Fig. 2, however, that the remaining diffraction lines do not split. Further increase of the magnetic field intensity leads to a redistribution of the intensity between the diffraction lines $(150)_r$ and $(310)_r$ (the former weakens, the latter becomes stronger) and a noticeable attenuation of the $(151)_r$ line[3].

In the ferromagnetic region, even without an applied magnetic field, the most intense diffraction peaks (the "former" hexagonal lines $(203)_h$ and $(210)_h$) are split into two components, since the crystal lattice has rhombic symmetry in this temperature range[4]. With increasing magnetic field intensity, an attenuation of the diffraction lines $(043)_r$ and $(151)_r$ is observed, as a result of which the diffraction pattern becomes similar to the x-ray pattern obtained at 145°K in a maximum field, although a noticeable redistribution of the intensities of the $(310)_r$ and $(150)_r$ lines, which take place at 145°K when $H \geq 12$ kOe, could not be observed even in a field of ~16 kOe.

In addition, at 77°K, a certain smearing of the diffraction maxima is observed with increasing magnetic field intensity, as a result of which the accuracy with which the positions of the peaks are determined is somewhat lower. The smearing of the lines was observed also at 145°K and $H > 10$ kOe.

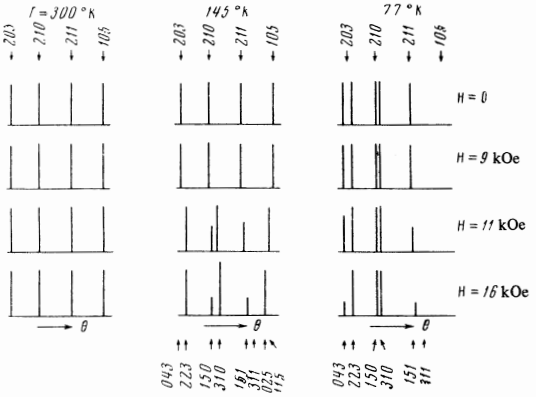

FIG. 2. X-ray patterns of dysprosium. The heights of the lines are proportional to the intensities of the x-ray reflection. The hexagonal indices are indicated on the top and the rhombic ones on the bottom.

In addition to the visual estimate of the intensities of the x-ray lines, we measured the interplanar distances as functions of the applied field. The curves

$$d_{(203)_h}(H) \text{ and } d_{(210)_h}(H) \text{ or } d_{(223)_r}(H),\ d_{(150)_r}(H) \text{ and } d_{(310)_r}(H)$$

were used to calculate the periods a, b, and c for the hcp or rhombic lattices of dysposium. The obtained field dependences of the lattice parameters are shown in Figs. 3 and 4.

In the paramagnetic region, the dependence of the periods a and c of the hcp lattice on the magnetic field intensity is quite weak, but a certain compression of the crystal lattice along the hexagonal axis is noticeable.

In the antiferromagnetic region, the dependence of the periods of the crystal lattice on the magnetic field intensity has a rather complicated character. Whereas the parameters a and c of the hcp lattice change quite little with the field in fields 0—9 kOe, a jumpwise lowering of the symmetry to rhombic takes place at $H = 10$ kOe (H_{cr}), as already noted. At $H > H_{cr}$, the period b increases noticeably with the field, while the period c decreases, and the period a changes insignificantly. The degree of rhombic distortion of the hcp lattice (b/a) naturally increases in this case (Fig. 5).

In the ferromagnetic region, no strong dependence of the period of the rhombic lattice on the magnetic field intensity is observed. The ratio of the periods (b/a) is practically independent of the field, and its

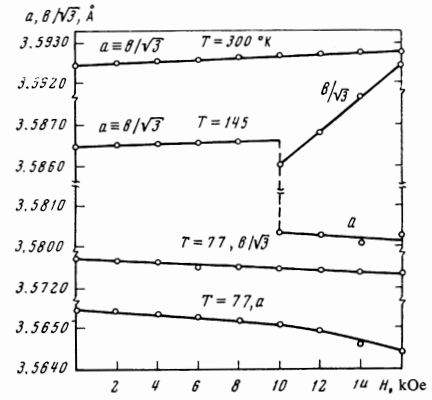

FIG. 3. Field dependence of the periods a and b.

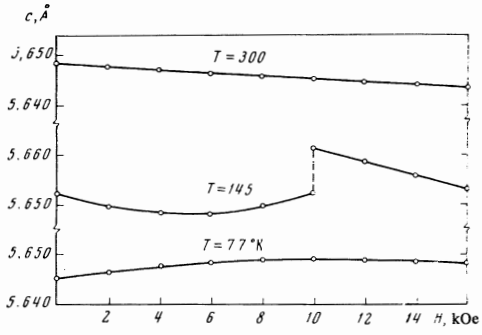

FIG. 4. Field dependence of the period c.

[2] The subscripts h and r stand for hcp and rhombic lattices.

[3] The geometry of the setup does not make it possible to register the line $(311)_r$, which is the second component of the split $(211)_h$ peak.